



Improved Directional Guidance with Transparent AR Displays

Felix P. Strobel¹^a and Voicu Popescu² ^b

¹Department of Informatics, Karlsruhe Institute of Technology, Karlsruhe, Germany

²Department of Computer Science, Purdue University, 305N University Street, West-Lafayette, U.S.A.

Keywords: Simulated Transparent Display, Robust Implementation, Augmented Reality.

Abstract: In a popular form of augmented reality (AR), the scene is captured with the back-facing camera of a hand-held phone or tablet, and annotations are overlaid onto the live video stream. However, the annotations are not integrated into the user's field of view, and the user is left with the challenging task of translating the annotations from the display to the real world. This challenge can be alleviated by modifying the video frame to approximate what the user would see in the absence of the display, making the display seem transparent. This paper demonstrates a robust transparent display implementation using only the back-facing camera of a tablet, which was tested extensively over a variety of complex real world scenes. A user study shows that the transparent AR display lets users locate annotations in the real world significantly more accurately than when using a conventional AR display.

1 INTRODUCTION


Augmented Reality (AR) is a powerful human-computer interface that allows overlaying computer-generated graphical annotations directly onto the user's view of the real world. The goal is to anchor the annotations to the real world elements that they describe, saving the user the cognitive effort of translating the annotations from a conventional computer display to the real world.


A popular implementation of AR interfaces relies on handheld AR displays: the user views the scene on a phone or computer tablet that shows a live video of the scene augmented with graphical annotations (Mohr et al., 2017; Grubert et al., 2014). Such AR displays have the advantages of being already mass deployed, of being familiar to most users, and of social acceptance. The disadvantages of AR displays include lack of depth cues, reduced field of view, and lack of true transparency.

Indeed, phones and tablets only *simulate* transparency by displaying the frame captured by the back-facing camera. Since the frame is captured from the camera's and not the user's viewpoint, and since the camera's field of view is different from the angle subtended by the display in the user's visual field, the frame is only a poor approximation of what the user

would see if the display were made of transparent glass. This results in redundancy and discontinuity between what the user sees *on* and what the user sees *around* the display (Pucihar et al., 2013). This dual-view problem makes conventional AR displays imperfect AR interfaces, as the annotations are not directly integrated into the user's view of the real world, but rather into the view of the back-facing camera. Therefore, AR displays do not completely relieve the user from the cognitive effort of translating the annotations from the computer display to their own view of the real world. A truly transparent display shows exactly what the user would see if the display were not there. Manufacturing transparent phones and tablets presents difficult technological challenges, as many components are opaque and large.

In order to modify the back-facing camera frame to match what the user would see in the absence of the AR display, two pieces of information are needed: the position of the user's head, and the geometry of the scene. Leveraging this information, the frame can be re-projected to the user's viewpoint using conventional projective texture mapping (Andersen et al., 2016). Prior work on simulating AR display transparency through user-perspective rendering has examined various modalities for tracking the user head and acquiring scene geometry, as well as approximations that bypass the need for this information. Some high-end tablets and phones can now track the

^a <https://orcid.org/0000-0002-2740-5169>

^b <https://orcid.org/0000-0002-8767-8724>

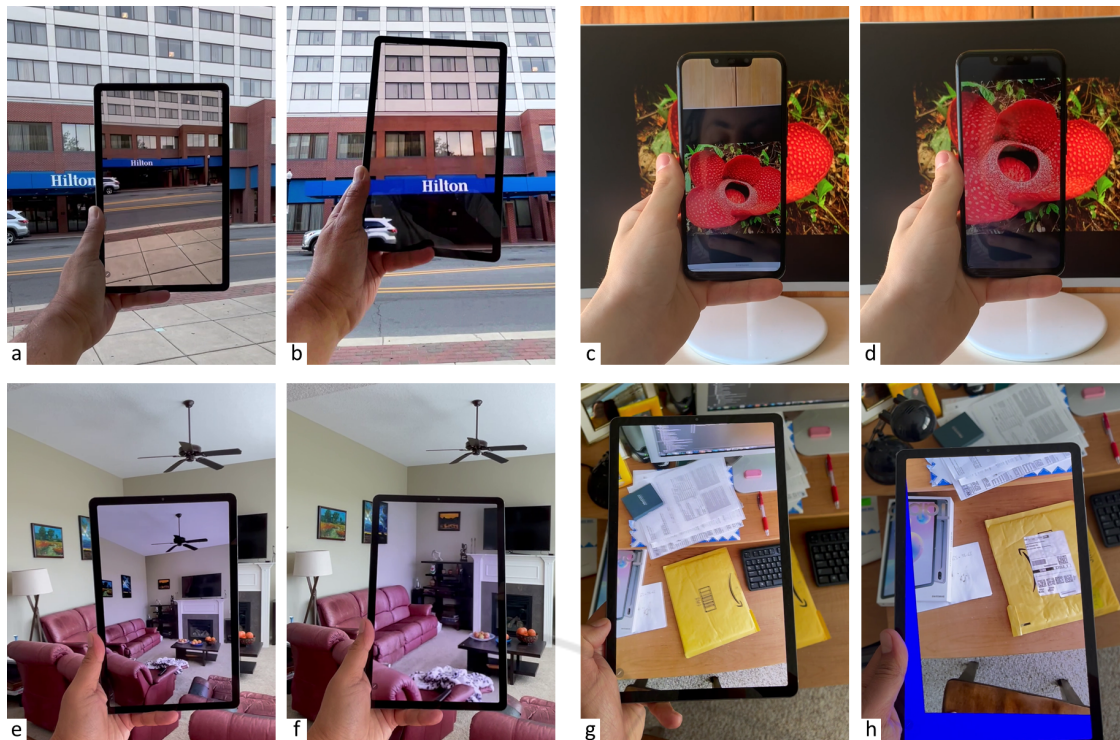


Figure 1: Conventional (left of each pair) and our transparent (right) AR display.

user’s head using the front-facing camera, and can acquire scene geometry actively using on-board depth cameras, or passively through structure-from-motion. However, no robust transparent AR display has yet been demonstrated and tested with users, and the AR displays used in practice continue to suffer from the dual-view problem.

In this paper we build upon prior work on user-perspective rendering to demonstrate a simulated transparent display that works robustly for a variety of complex scenes, that is implemented with a simple phone or tablet with just a back-facing camera, and that improves the directional guidance provided to the user. The design of our transparent display is anchored by two considerations.

First, we argue that for some AR applications the computational or hardware expense of tracking the user’s head is unnecessary; indeed, as the user examines various parts of the scene, they are likely to move their head and arm together, holding the phone or tablet in a little-changing ergonomic sweet spot, much the same as when photographing or video recording a scene; the user naturally holds the phone to see it straight on, avoiding skewed viewing angles. Since the user can comfortably hold the display in a stable sweet spot, it is reasonable to expect their cooperation, and not be concerned about adversarial behavior—the point is not that a user could easily break

the illusion of transparency by looking at their phone at a shallow angle, but rather that the user could easily hold it such that transparency works to provide accurate directional guidance. Furthermore, in some AR applications such as driver assistance, the user’s head is naturally at a constant position relative to the display.

Second, we argue that robust, complete, and real time scene geometry acquisition will not be tractable in the near future, and therefore suitable scene geometry approximations *have* to be found to allow handheld AR reach its potential for wide adoption. Acquiring quality depth of a dynamic scene with intricate geometry, such as a water fountain or a leafy tree swaying in the wind remains a challenging technological problem; furthermore, even if future generation phones or tablets acquire perfect depth for such challenging scenes, the depth acquired from the device perspective might not be enough, as the user could see parts of the scene that are occluded from the device perspective.

Based on these considerations, we have devised our AR display (1) to cater to a fixed user viewpoint, and (2) to map the frame to the user view through a homography defined either by a planar proxy of the scene geometry, or by the distant geometry assumption. Our AR display is robust, avoiding the objectionable artifacts caused by user head tracking or

scene geometry acquisition errors.

Fig. 1 illustrates the improved transparency achieved by our AR display, compared to a conventional AR display. The transparent AR display was implemented with the distant geometry assumption for examples (b) and (f) and with the planar proxy assumption for (d) and (h). The distant geometry assumption works well even for the living room scene (f) where scene geometry is between one and five meters away from the user. In (h), the desk is close to the large tablet and some parts of the scene (blue) occluded by the tablet and hence needed for the transparency effect were not captured by the tablet’s back-facing camera; in (d) the camera of the (smaller) phone captures all needed pixels. Our AR display achieves good transparency, which improves directional guidance. Consider an AR application that indicates a specific window by circling it on the façade shown in (a) and (b); the transparent display (b) will place the circle correctly on the line connecting the user viewpoint to the actual location of the window in the real world, providing the user with the true direction to the window of interest; on the other hand, the conventional display (a) does not directly point to the location of the window in the real world; the user has to study the visualization closely to memorize the location of the window relative to unique visual features and then to translate the memorized location from the visualization to the real world.

We have compared our transparent AR displays to conventional AR displays both analytically and empirically, for a variety of complex scenes, and the results show that our displays have superior transparency accuracy. We have also conducted a controlled user study ($N = 17$), which showed that, compared to a conventional AR display, our transparent AR display reduced annotation localization error by a statistically significant 61%. Our transparent AR display is robust, ready to be enrolled in AR applications. We also refer the reader to the accompanying video.

In summary, our paper makes the following contributions:

- The design of a practical transparent AR display, validated analytically and empirically.
- The implementation of a robust transparent AR display prototype that produces a quality transparency approximation regardless of scene complexity, motion, and lighting conditions.
- A controlled user study that confirms the superior directional guidance afforded by the proposed transparent AR display.

2 PRIOR WORK

The holy grail of AR interfaces is an HMD in the form factor of regular vision glasses or even contact lenses. Whereas considerable progress has been made, optical see-through AR HMDs remain bulky, expensive, with a limited field view, dim, and without the ability to render with full opacity. Therefore, researchers have been exploring an alternative AR interface, where the user holds a simulated transparent display that overlays graphical annotations onto the scene.

An early implementation uses a head-mounted projector and a handheld screen, which, despite the user encumbrance, demonstrates the feasibility and benefit of a handheld simulated transparent display (Yoshida et al., 2008). Subsequent AR transparent displays leverage portable active displays with built-in cameras. One challenge is to register the display in the user’s frame, which was addressed with a camera mounted on the user’s head (Samini and Palmerius, 2014; Baričević et al., 2012), or with a camera mounted on the handheld display and aimed at the user (Baričević et al., 2017; Grubert et al., 2014; Hill et al., 2011; Matsuda et al., 2013; Tomioka et al., 2013; Uchida and Komuro, 2013; Zhang et al., 2013; Andersen et al., 2016).

A second challenge is to acquire the scene geometry and color in real time. Several simulated transparent display prototypes work under the assumption that the scene is planar. The planar scene proxy is either precalibrated (Matsuda et al., 2013; Zhang et al., 2013), or tracked using markers added to the scene (Grubert et al., 2014; Hill et al., 2011; Samini and Palmerius, 2014; Uchida and Komuro, 2013) or using scene features (Tomioka et al., 2013). Other researchers have opted for per-pixel depth acquisition, with on-board depth cameras (Baričević et al., 2012; Andersen et al., 2016), or through structure from motion (Baričević et al., 2017). The planar scene proxy approach has the advantage of greatly simplifying depth acquisition, and of hiding disocclusion errors. The per-pixel depth approach has the potential for more accurate transparency as the scene geometry is captured with greater fidelity, but is hampered by artifacts due to depth acquisition imperfections, and to disocclusion errors due to parts of the scene visible from the user viewpoint but not from the camera viewpoint.

Another goal in transparent AR display development was untethering the device to achieve complete portability. Whereas early prototypes required wire connections to power sources, trackers, or workstations, the advances of smartphone and com-

puter tablet technology has enabled compact, self-contained handheld AR displays (Grubert et al., 2014; Matsuda et al., 2013; Samini and Palmerius, 2014; Zhang et al., 2013; Baričević et al., 2017; Baričević et al., 2012; Andersen et al., 2016).

The dual-view problem was noted early on in studies that showed that users expect the display to simulate transparency accurately (Pucihar et al., 2013). Early prototypes assumed a fixed user viewpoint (Pucihar et al., 2013), and subsequent prototypes investigated tracking the user head. One system (Mohr et al., 2017) tracks the user head with a front-facing camera. To make the computational cost tractable, the user head is not tracked every frame. Even so, the computational demand exceeded what the phone could sustain and the user study was conducted on a PC workstation. The study revealed that users perform better in a fixed-viewpoint condition compared to the full head tracking condition, and the difference was attributed to head-tracking failures.

Researchers have analyzed the potential of planar approximations of scene geometry (Borsoi and Costa, 2018), but they did not consider the distant geometry ("plane at infinity") approximation; furthermore, the proposed approximations were not implemented on a portable AR display, and they were not tested with users. We show that the distant geometry based homography yields good results even for scenes a few meters away from the user, bypassing scene geometry acquisition altogether. Furthermore, we have implemented our design in a robust prototype which we have user tested successfully.

Our work is inspired by that of Andersen et al. (Andersen et al., 2016), who examined the feasibility of transparent AR display implementation by taking advantage of emerging features of phones and tablets. They describe three transparent AR display prototypes. One prototype leverages hardware user tracking provided by a phone with four front-facing cameras, one at each display corner. A second prototype leverages the on-board depth camera of a computer tablet to capture the scene geometry. A third prototype combines the other two prototypes to achieve both user tracking and scene geometry acquisition. The two prototypes that rely on depth acquisition suffer from objectionable artifacts due to depth and disocclusion errors. The prototypes are not tested with users. Our work provides analytical and empirical evidence that transparent AR displays can be implemented with *any* phone or tablet, *without* the prerequisites of advanced features such as user tracking or depth acquisition, and we demonstrate the improved directional guidance achieved by our transparent AR display in a user study.

3 SIMULATING AR DISPLAY TRANSPARENCY

Since truly transparent tablets and phones are not yet feasible, one is left with simulating transparency in video-see-through fashion, leveraging the back-facing camera that captures the scene in real time. One option is to simply display the camera frames as is. This is the option currently taken by most if not all AR applications, and we refer to this option as the *conventional* AR display. Since the user viewpoint is different from that of the camera, the transparency effect can be improved by reprojecting the camera frame to the user viewpoint. Reprojecting the frame to the user viewpoint requires (1) knowledge of the 3D scene geometry, as the reprojection includes a translation from the camera to the user viewpoint, and requires (2) knowledge of the user viewpoint, as what the user sees through an ideal glass-like transparent AR display depends on where the user's head is with respect to the display.

(1) Recent high-end phones have some depth acquisition capability. However, real time depth acquisition of scenes with intricate or dynamic geometry, such as a leafy plant swaying in the breeze, or of scenes with complex reflective properties, such as a water fountain, remains challenging. Furthermore, even if the back-facing camera acquires perfect per-pixel depth, the resulting simulated transparency might still suffer from severe artifacts due to occlusions. In Fig. 2a, reprojecting to U the color and depth acquired from C results in artifacts due to the missing samples of the left face of the box. In other words, accurate transparency requires quality and robust real-time depth acquisition from not one, but from *multiple* viewpoints. We submit that depth acquisition can be bypassed altogether by mapping the camera image to the user image with a homography, which results in a quality simulated transparency approximation, as we show analytically and empirically in the following sections.

(2) Recent high-end tablets and phones also provide user-head tracking, leveraging on-board sensors that are aimed at the user (front-facing). These additions are motivated by the popularity of AR enhancements of video conferencing applications, such as modifying the appearance of the speaker by changing their facial features or by attaching graphics to the speaker's head. Such applications require tracking the user's head with six degrees of freedom. However, for our application of transparent AR displays, only the three translations that place the user's head with respect to the display are needed, because the rotations do not change what the user sees through the display

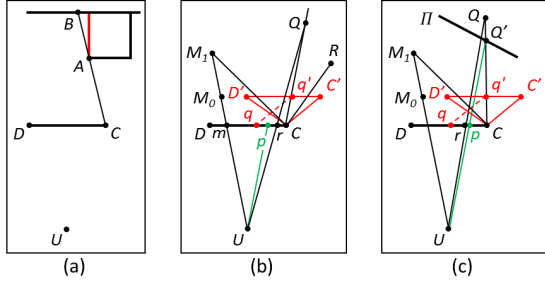


Figure 2: (a) Disocclusion artifacts. The left side of the box (red) is missed by the back-facing camera C located at the corner of the AR display DC , but is visible from the user viewpoint U . Even with perfect depth, reprojecting to U a color and depth frame acquired from C results in disocclusion artifacts. (b) AR display transparency with the distant geometry assumption. A pixel p is looked up in camera frame $D'C'$ along a ray from C with direction Up , setting it to the color at q' . (c) AR display transparency with the planar proxy geometry approximation. A pixel p is looked up in camera frame $D'C'$ by projecting its proxy point Q' to q' .

frame. Furthermore, in video conferencing applications the user frequently moves their head with respect to the tablet or phone. This is especially true in the common use case when the device is placed in a bracket that anchors it to the scene (e.g., tabletop, car dashboard), and not to the user. However, in transparent display AR applications the user typically holds the display at a fixed position with respect to their head, moving the display as they pan and tilt their view direction, much the same way they hold the display when it serves as a viewfinder when taking photos. We submit that user head tracking can be bypassed altogether by assuming that the user’s head is in a default position, which results in a quality simulated transparency approximation, as we show analytically and empirically in the following sections.

3.1 Geometric Accuracy of AR Display Transparency

We first define three measures of AR display transparency error which we then use to quantify the quality of our AR transparent display approximations. Please also refer to Fig. 3.

Reprojection Error ϵ . Given a 2D point p on an approximate transparent display that shows 3D scene point P , the reprojection error ϵ at p is defined with Fig. 2, where q is the projection of P on a perfectly accurate transparent display. In other words, pixel p is ϵ away from its true position.

$$\epsilon = \|p - q\| \quad (1)$$

The reprojection error ϵ is measured in pixels and it can be converted to units of length, e.g., mm, by taking into account the physical size of the display. The reprojection error can also be measured in degrees, as the size of the angle between the user rays through p and q , which indicates how far off the direction indicated by the AR display is from the true direction in the real world scene. We quantify the reprojection error over the entire transparent display as the average and maximum reprojection errors over all pixel centers.

Number of Missing Pixels μ . Another measure of the difference between the image I^* shown by an approximate transparent display and the image I shown by a perfectly accurate transparent display is the number μ of pixels in I that are missing from I^* . We express μ as a percentage from the total number of pixels in I , to make it resolution independent. There are three types of missing pixels: (1) pixels not captured by the camera because they correspond to 3D scene points outside the camera’s view frustum, like the blue pixels in Fig. 1h; (2) pixels not captured by the camera because they correspond to 3D scene points that *are* inside the camera’s view frustum but are not visible to the camera due to occlusions (Fig. 2a); and (3) pixels captured by the camera but incorrectly discarded by the transparency approximation.

Number of Redundant Pixels ρ . Another measure of the difference between the image I^* shown by an approximate transparent display and the image I shown by a perfectly accurate transparent display is the number ρ of pixels in I^* that are missing from I , i.e., pixels that should not be part of I^* . These pixels correspond to parts of the scene that the user sees directly, around the display, and they are shown redundantly on the approximate transparent display, creating a double vision artifact. We express ρ as a percentage from the total number of pixels in I^* , to make it resolution independent. In Fig. 1e, the pixels of the ceiling fan are redundant as the fan is directly visible to the user above the display.

3.2 Homography-based AR Display Transparency

Connecting the camera and user views using a homography allows modifying the frame acquired by the camera to better approximate what the user would see through a perfectly transparent display, while bypassing depth acquisition, and while avoiding artifacts due to occlusions. Using Fig. 2a again, repro-

jecting the frame with a homography, which is a bijective mapping, keeps the projection of points A and B at the same display location, preventing the disocclusion error gap from forming. We have investigated two options for defining the homography between the user and camera views.

3.2.1 Distant Geometry Assumption

The first option is to assume the scene geometry is far away from the display, which allows ignoring the distance between the camera viewpoint and the user viewpoint. In Fig. 2b, the AR display DC has a back-facing video camera at C , with frustum $D'CC'$. Transparency is approximated by mapping each display pixel p to the camera frame based solely on the direction of the pixel's ray Up .

A transparent display pixel (u, v) is mapped to the camera frame as follows. First, the 3D point p corresponding to pixel center is computed with Fig. 2, where the user view frustum (i.e., DUC in Fig. 2) is encoded as a planar pinhole camera with the eye at the user viewpoint U , with row and column vectors a_u and b_u , and with eye to top left image corner vector c_u . We use column vectors.

$$p = U + [a_u \ b_u \ c_u] [u \ v \ 1]^T \quad (2)$$

Then ray Up is translated to C and its tip is projected with the camera to obtain the frame mapping (u_q, v_q) , using Fig. 3.

$$C + p - U = C + [a_c \ b_c \ c_c] [u_q w_q \ v_q w_q \ w_q]^T \quad (3)$$

The 3D vector Fig. 3 has three scalar equations, i.e., one for each of the three dimensions x , y , and z , and three unknowns, i.e., u_q , v_q , and w_q , which are found by solving as shown in Fig. 4.

$$[u_q w_q \ v_q w_q \ w_q]^T = [a_c \ b_c \ c_c]^{-1} (p - U) \quad (4)$$

The reprojection error ϵ_d introduced by the distant geometry assumption is computed as follows. Given pixel p , the transparent display sets it to the color of the camera frame at q' , where the camera captured the 3D scene point Q . The true projection of Q on the transparent display is at r , so $\epsilon_d = \|p - r\|$. The conventional AR display, which shows the camera frame as is, projects Q at q , which has the same image coordinates as q' , for a reprojection error of $\epsilon_c = \|q - r\|$. As can be seen in Fig. 2b, even for a 3D scene point Q that is fairly close to the display, the transparency achieved with the distant geometry assumption improves over the conventional transparency, i.e., $\epsilon_d < \epsilon_c$. As expected, the transparency

error decreases as the distance to the scene increases. As Q moves farther from C on Cq' , r moves closer to p , reducing ϵ_d , while ϵ_c stays the same. At the limit, the distant geometry assumption yields a perfectly accurate transparent display (Fig. 5).

$$\lim_{Q \rightarrow \infty} \epsilon_d = 0, \lim_{Q \rightarrow \infty} \epsilon_c = \|p - q\| \quad (5)$$

Our transparent display has missing pixels. One example is the pixel corresponding to M_0 in Fig. 2b, which was not captured by the camera, and is therefore missing from the conventional AR display as well. Another example is the pixel corresponding to M_1 , which is captured by the camera but it is discarded since the direction CM_1 is beyond the left boundary DU of the user view frustum.

Even for large tablets (e.g., 50cm), the angle subtended by the display in the user's field of view (e.g., 53° at 50cm) is smaller than the field of view of the camera. Therefore, the reprojection implemented using the distant geometry assumption is essentially a zoom in operation. As such, our transparent display does not have redundant pixels. Consider a 3D scene point that the user sees directly, beyond the display, e.g., R in Fig. 2b. A ray from U with direction CR is to the right of CU , so R does not appear on the transparent display. The conventional AR display *does* have redundant pixels: R is captured by the camera and hence shown on the display, in addition to being seen directly by the user.

3.2.2 Analysis of Distant Geometry Assumption

We have analyzed our transparent display based on the distant geometry assumption and we have compared it to a conventional AR display using a software simulator (Fig. 3). The simulator models a 23cm \times 14cm tablet (10.5inch diagonal) with an 80° back-facing camera at its top right corner. These parameters correspond to the wide angle back camera of a Samsung Tab6 (Fig. 1) The user views the tablet perpendicularly to its center from a distance of 50cm. The 3D scene is a vertical wall texture mapped with the photograph of a painting. The wall is pushed back to various distances, while scaling up the painting to keep the user's view of the real world unchanged. The scaling has no effect on the performance of either display, it is done for illustration eloquence. The distant geometry assumption works well even when the scene is 2m away from the display, where it improves the transparency effect over the conventional display by removing the redundant pixels and by reducing the reprojection error. The largest errors are at the left and bottom edges of our transparent display, which are farthest from the top-right camera. At 5m, the visu-

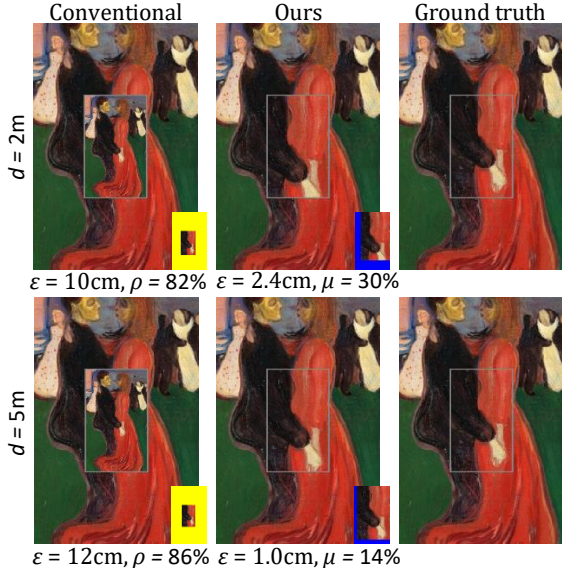


Figure 3: Software simulator comparison between three AR displays: a conventional one that shows the camera frame as is, ours based on the distant geometry assumption, and ground truth with perfect transparency. The bottom right vignettes show the redundant (yellow) and missing (blue) pixels. Our display improves over the transparency of the conventional display even at 2m, and, at 5m, our display transparency is close to ground truth.

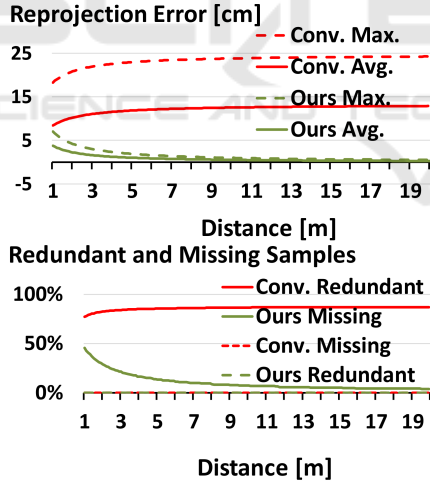


Figure 4: **(Top)** Average and maximum reprojection errors for the conventional and the distant geometry transparent AR displays, as a function of scene distance. **(Bottom)** Missing and redundant pixels for the conventional and the distant geometry transparent displays, as a function of scene distance.

alization discontinuity across the frame of the display is barely noticeable. The reprojection error and the redundancy of the conventional AR display are large, and they increase with distance.

Fig. 4, left, shows that our transparent display

has smaller maximum and average reprojection errors compared to the conventional AR display for any display to scene distance beyond 1m. At 2m, 3m, 5m, 10m, and 20m, the average reprojection error for our display is 2.4cm, 1.7cm, 1.0cm, 0.54cm, and 0.27cm. Using the 50cm user viewpoint distance, these translate to directional errors of 2.7°, 1.9°, 1.1°, 0.6°, and 0.3°. The conventional display has large and growing average reprojection errors of over 10cm (11°). Fig. 4, right, shows that no matter the distance to the scene, our transparent display has no redundant pixels, and that the percentage of missing pixels decreases with distance. The conventional AR display has no missing pixels, but over 80% of its pixels show the user a part of the real world that they already see directly, around the display.

3.2.3 Planar Proxy Geometry Approximation

The second option we have investigated is to build the homography by approximating the scene geometry with a plane. In Fig. 2c the scene planar proxy is Π . Transparency is approximated by mapping each display pixel (u, v) to the camera frame by computing the pixel center 3D point p using Fig. 2, by computing the intersection Q' of ray Up with Π by solving the system Fig. 6 where n and p_0 are the normal and a point of Π , and by projecting Q' with the camera to frame point (u_q, v_q) using Fig. 7.

$$n(p_0 - Q') = 0 \quad (6)$$

$$Q' = U + (p - U)w_q$$

$$\begin{bmatrix} u_q w_q & v_q w_q & w_q \end{bmatrix}^T = \begin{bmatrix} a_c & b_c & c_c \end{bmatrix}^{-1} (Q' - C) \quad (7)$$

Since the proxy is only an approximation of the scene geometry, the 3D scene point captured by the camera at q' is Q and not Q' , which translates to a reprojection error $\epsilon_p = \|p - r\|$, where r is the projection of Q onto DC as seen from U . The closer a 3D scene point is to the proxy, the smaller its reprojection error; points on the proxy have a reprojection error of 0. The farther the geometry, the less impact a given out-of-proxy displacement has, due to perspective foreshortening. Like before, conventional AR display projects Q to q for a reprojection error $\epsilon_c = \|q - r\|$.

Like the distant geometry display, the planar proxy display can have missing pixels, e.g., M_0 in Fig. 2c, which was not captured by the camera, and M_1 , whose proxy point is outside the user view frustum as Π intersects CM_1 to the left of UD . Unlike the distant geometry display, the planar proxy display can have redundant pixels. In Fig. 5a, the 3D scene

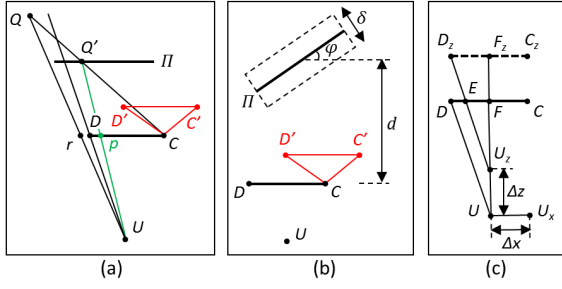


Figure 5: (a) Redundancy example for planar proxy transparent display: point Q is seen directly by the user as ray UQ is not blocked by the display DC , and it also appears on the transparent display at p . (b) Simulator setup for the analysis of the planar proxy geometry approximation. (c) User viewpoint deviation from assumed position U .

point Q is seen by the user directly as its projection r is outside the display DC . However, the corresponding proxy point Q' projects inside the display at p , so the user also sees Q on the display, redundantly.

3.2.4 Analysis of Planar Geometry Assumption

We have analyzed the quality of the transparent display obtained with the planar geometry assumption using a simulator configured as shown in Fig. 5b. The proxy plane Π is at distance $d = 1\text{m}$ from the display DC , it is vertical, and it makes an angle $\phi = 45^\circ$ with the display plane. The actual 3D scene has a displacement out of the proxy plane between $+\delta/2$ and $-\delta/2$, with $\delta = 50\text{cm}$. In summary, when the scene is farther than the proxy, i.e., $\delta = -25\text{cm}$, our display has a few redundant pixels, and no missing pixels; when the scene is closer than the proxy, i.e., $\delta = 25\text{cm}$, our display has no redundant pixels, and a few missing pixels. In all cases, our display provides acceptable transparency, i.e., there is good visualization continuity across the display frame. The conventional display suffers from substantial redundancy and provides a poor transparency effect. The planar proxy display has a small reprojection error, which decreases as the quality of the geometry approximation provided by the proxy increases. The planar proxy display has a smaller reprojection error than the conventional display.

3.3 Default Head Position AR Display Transparency

We propose to implement transparent displays by bypassing user head tracking, under the assumption that the user viewpoint is in a default position. Since in practice the user viewpoint will deviate from the default position, we now analyze the implications of such deviations on the reprojection error.

Given an actual user viewpoint U^* that is assumed to be at U , the component of the U^*U translation vector parallel to the display is added directly to the reprojection error, shifting up by Δx the graphs given in Fig. 4. In Fig. 5c the actual user viewpoint U_x is to the right of the assumed viewpoint U and the transparent display reprojection error ε increases by Δx . The reprojection error is typically less sensitive to the translation vector component perpendicular to the display. In Fig. 5c, when the actual user viewpoint is at U_z , the reprojection error increases by DE , which is given by Fig. 8, where w is the width of the display and f is the distance from the default user viewpoint to the display. As long as $f > w/2$, the reprojection error increase is less than the deviation in z , i.e., Δz . For the large 10inch tablet used in the simulator, f is 40cm, and w is 14cm in portrait mode and 23cm in landscape mode, so $f \gg w/2$. For smaller displays, e.g., a phone, the reprojection error is even less sensitive with the z component of the user head position.

$$\begin{aligned} \|DE\| &= \|DF\| - \|EF\| = \\ &= \|DF\| - \|D_z F_z\| \|U_z F\| / \|U_z F_z\| = \quad (8) \\ &= w/2 - (w/2)(f - \Delta z)/f = (w\Delta z)/(2f) \end{aligned}$$

4 EMPIRICAL RESULTS AND DISCUSSION

We have tested our transparent AR displays on a variety of scenes, where they proved to be robust with scene geometry complexity, and with displacements of the handheld display away from the assumed default position, see Fig. 1, Fig. 6, Fig. 7, and accompanying video.

Fig. 6 confirms the results of our theoretical analysis of the approximation error introduced by the distant geometry assumption: even when the geometry is relatively close to the user, our transparent display based on the distant geometry assumption produces good transparency results. Fig. 7 shows that our transparent display works for dynamic scenes, for which it preserves the continuity of the trajectory of moving objects (also see accompanying video). In frame b, the half of the passing car shown on the display is well aligned with its other half that the user sees directly, around the display.

We have conducted a within-subjects controlled user study ($N = 17$) to quantify any potential directional guidance benefits of our transparent AR display, compared to a conventional AR display.

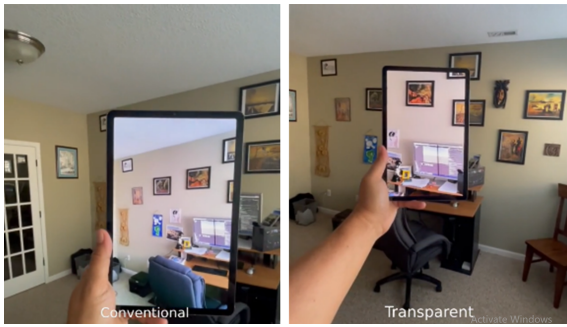


Figure 6: Comparison between a conventional AR display (left) and our transparent display based on the distant geometry assumption (right). Although the desk is less than 2m away, there is little visualization discontinuity between the display and its surroundings.

4.1 Study Design

General Procedure. The essence of our user study procedure is to show the participant an annotation on the AR display, and then to ask the participant to indicate the location of the annotation in the real world. An important concern is to record the real world location indicated by the participant accurately, such that it can be compared with the known correct location of the annotation. To achieve this, we designed a procedure where the participant is seated in front of a laptop (Fig. 8); the transparent AR display is implemented with a phone (left); the participant holds the AR display in their hand and looks through it at a laptop screen which displays an image; the AR display annotates the image shown by the laptop with a dot; the annotation is shown for 2s; once the annotation disappears, the participant is asked to indicate the position of the annotation on the laptop screen using the mouse; this way, the location indicated by the participant can be recorded accurately by the laptop. The display transparency is computed in the planar proxy mode, leveraging the planarity of the laptop screen.

Participants. We recruited 17 participants from a high school, including students and teachers, with ages between 16 and 52, 12 male and 5 female. The study was approved by the institution, and was conducted with informed consent from participants or their legal guardians. We asked participants to rate their prior experience with AR applications; 4 partici-



Figure 7: Transparent display frames with passing car moving from being seen on transparent display (a) to being seen directly (c).

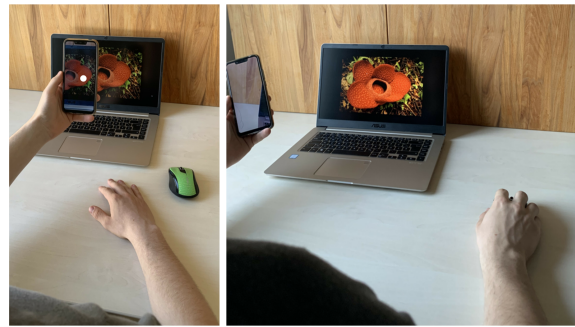


Figure 8: Experimental setup: (left) annotation (white dot, enlarged here for illustration clarity) shown to participant through our transparent AR display implemented with handheld phone, and (right) participant indicating the annotation location using mouse.

pants rated their AR experience as high, 6 as medium, 2 as low, and 5 as none. The participant AR experience was related to the use of applications such as Pokémon GO and Snapchat.

Conditions (Independent Variable). The study had two conditions. In a first, control condition (CC), the AR display showed the annotation directly on the video frame captured by the phone’s back-facing camera (i.e., conventional AR display). In a second, experimental condition (EC), the AR display showed the annotation with improved transparency, based on tracking the planar image displayed on the workstation screen (i.e., our transparent AR display).

Implementation Details. We implemented the AR display as an Android app deployed on a HUAWEI Mate20 lite phone. The phone was held in portrait mode. The phone screen is 14.7cm tall and 6.4cm wide. The application was developed in Unity version 2020.3.2 using AR Foundation, which builds upon Google’s AR Core.

The EC condition was implemented with a fragment shader that looks up each AR display pixel in the original frame using conventional projective texture mapping between the user view and the back-facing camera view, which are connected by the homography defined by the tracked laptop image plane. The annotation location was mapped using a similar projective texture mapping operation that unprojects the original frame coordinates to 3D on the tracked image plane and then projects the 3D position onto the AR display. The CC condition was implemented with a fragment shader that places the dot directly on the original frame, leveraging the tracked laptop image plane.

For the planar proxy mode, the plane is tracked up to a constant of proportionality, as is always the case in passive computer vision algorithms. In other words, the transparency effect works the same for a

plane that is twice as big and is twice as far away. There are no parameters that need to be set.

The laptop displays the image which is annotated by the AR display, and it runs a simple data collection application that records the mouse clicks for every annotation localization task.

Tasks. Each participant performed 10 annotation localization tasks for the CC condition and 10 for the EC condition (within-subject design). The condition order was randomized. As described above, the annotation localization task shows the user an annotation on the phone anchored to the image displayed by the laptop, and then asks the user to indicate the location of the annotation on the laptop screen using the laptop’s mouse.

Dependent Variable. For each task, the workstation measured the annotation localization error as the distance in pixels between the correct and the participant indicated locations.

Data Analysis Procedure. The localization errors of the two conditions were compared using a dependent T-Test, as required by our within-subject design, and using effect sizes quantified with Cohen’s d (Cohen, 1988). We used the SPSS statistical software package.

4.2 Study Results and Discussion

Fig. 9, left, shows the box plots of the localization error, for each of the two conditions. The mean localization error in pixels was 23.94 ± 6.35 for CC and 9.24 ± 2.68 for EC. Using the size of the image on screen and the distance from the participant to the screen, these localization errors correspond to angular errors of $0.46 \pm 0.12^\circ$ for CC and $0.18 \pm 0.05^\circ$ for EC. The mean error difference CC-EC was 14.71 ± 4.90 pix, and $0.28 \pm 0.07^\circ$. The scatter plot in Fig. 9, right, illustrates the actual participant click locations around the true annotation position, in pixels—the errors appear uniformly distributed around the correct location, with a higher error magnitude for CC.

The four assumptions of the dependent T-Test hold: our dependent variable is continuous, there are two dependent groups, there were no significant outliers in the differences between the two groups, and the differences in the dependent variable between the two related groups are normally distributed, which we verified ($p = 0.520$) using the Shapiro-Wilk test (Shapiro and Wilk, 1965). The dependent T-Test shows that the experimental condition localization errors are significantly lower than the control condition errors ($t(16) = 12.384, p < 0.0005$). We measured the effect size using Cohen’s d , which revealed a *Huge* (Sawilowsky, 2009) effect size ($d = 3.004$).

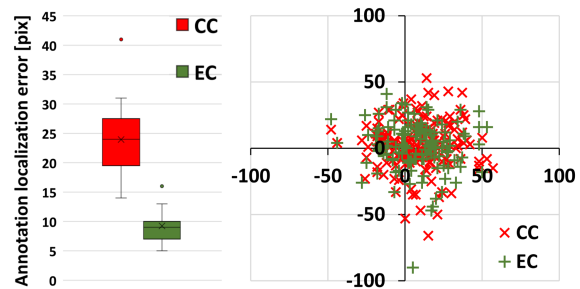


Figure 9: Box and scatter plots of annotation localization errors for the control (CC) and experimental (EC) conditions.

The study results indicate a significant advantage for our transparent display in terms of annotation localization accuracy, compared to the conventional AR display. Our transparent display places the annotation at a more accurate location in the user’s field of view, and the user can extrapolate its location from the display to the real world with significantly higher accuracy. On the other hand, the conventional AR display requires the user to estimate the position of the annotation in the real world based on memorized landmarks, which is challenging.

We note that the flower image used in our study (Fig. 8) is not repetitive and it does have salient features, which makes the annotation localization tractable for the conventional AR display. Annotation localization can become more difficult with the conventional AR display for texture-less or repetitive images. For example, the user is unlikely to find a specific window in a façade using the conventional display, as all windows look the same (Fig. 1a).

5 CONCLUSIONS AND FUTURE WORK

We have described an AR display with good transparency accuracy for a variety of scenes with complex and dynamic geometry. Transparency accuracy is robust to deviations of the user viewpoint away from the assumed default position, and to non-planar or close-by scene geometry. A study shows that our transparent display lets users locate annotations in the real world with significantly higher accuracy, by eliminating the landmark memorization and annotation remapping tasks of conventional AR displays.

The handheld display AR interface makes use of devices such as phones and computer tablets, which have many of the AR required qualities, such as a high resolution back-facing camera, a high resolution display, and a compact form factor. However, these devices were not designed for AR, and they have lim-

itations that our AR displays inherit. One is that the camera is typically placed at the corner and not at the center of the display, which translates to more missing pixels for the planar geometry transparent AR display when the scene geometry is close (Fig. 1h). A second limitation is the latency between frame capture and display. Whereas this is acceptable when the display is used as a camera viewfinder, the latency is problematic in AR where it causes annotations to drift as the display moves. In our specific context, latency makes the transparency accuracy lag when the display moves abruptly (see driving sequence in video accompanying our paper). Future work could examine leveraging motion prediction or low latency sensors such as the display's accelerometers to try to alleviate this latency, but the more robust solution is likely to require that the latency be eliminated by phone and tablet manufacturers.

In its current implementation, the user is asked to choose between the two modes: planar proxy or distant geometry. For the planar proxy mode, the system assumes that it sees only plane. Future work could look into actively searching for planes and for switching between the two modes on the fly, as needed, without user intervention. Our display transparency works best when the user head position is indeed at the default distance above the center of the display. Holding this position reasonably well is possible, as shown by the video and by the results of our study. Future work could examine giving the user cues about their head position, which is easier to do than full head tracking.

Another limitation that our approach inherits from the conventional AR display interface is the lack of depth cues. Whereas with a truly transparent display the scene is seen stereoscopically, and therefore it appears at the correct depth, the transparent display provides a monoscopic view of the scene, at a fixed, nearby distance. Even though one has to change focus from the nearby display to the scene, our study participants have been able to extrapolate the direction of the annotation to map it to the scene more accurately when using our transparent display, compared to when using the conventional AR display, which is also void of depth cues.

Our approach for improving AR display transparency has the advantage of working on any phone or tablet with a back-facing camera, without requiring depth acquisition or user tracking capabilities. Furthermore, the computational cost of the homography is low, so our approach is compatible even with low end devices. Our approach brings an infrastructure-level contribution that is ready to be integrated in virtually all AR applications, where it promises the ben-

efit of improved directional guidance.

ACKNOWLEDGEMENTS

We thank our participants for their essential role in validating our work. We thank Andreas Schuker and Susanne Goedicke for all their support. We thank the anonymous reviewers for their help with improving this manuscript.

REFERENCES

- Andersen, D., Popescu, V., Lin, C., Cabrera, M. E., Shaghavi, A., and Wachs, J. (2016). A hand-held, self-contained simulated transparent display. In *2016 IEEE International Symposium on Mixed and Augmented Reality (ISMAR-Adjunct)*, pages 96–101.
- Baričević, D., Höllerer, T., Sen, P., and Turk, M. (2017). User-perspective ar magic lens from gradient-based ibr and semi-dense stereo. *IEEE Transactions on Visualization and Computer Graphics*, 23(7):1838–1851.
- Baričević, D., Lee, C., Turk, M., Höllerer, T., and Bowman, D. A. (2012). A hand-held ar magic lens with user-perspective rendering. In *2012 IEEE International Symposium on Mixed and Augmented Reality (ISMAR)*, pages 197–206.
- Borsoi, R. A. and Costa, G. H. (2018). On the performance and implementation of parallax free video see-through displays. *IEEE Transactions on Visualization and Computer Graphics*, 24(6):2011–2022.
- Cohen, J. (1988). *Statistical power analysis for the behavioral sciences*. Hillsdale, N.J.: L. Erlbaum Associates.
- Grubert, J., Seichter, H., and Schmalstieg, D. (2014). [poster] towards user perspective augmented reality for public displays. In *2014 IEEE International Symposium on Mixed and Augmented Reality (ISMAR)*, pages 267–268.
- Hill, A., Schiefer, J., Wilson, J., Davidson, B., Gandy, M., and MacIntyre, B. (2011). Virtual transparency: Introducing parallax view into video see-through ar. In *2011 10th IEEE International Symposium on Mixed and Augmented Reality*, pages 239–240.
- Matsuda, Y., Shibata, F., Kimura, A., and Tamura, H. (2013). Poster: Creating a user-specific perspective view for mobile mixed reality systems on smartphones. In *2013 IEEE Symposium on 3D User Interfaces (3DUI)*, pages 157–158.
- Mohr, P., Tatzgern, M., Grubert, J., Schmalstieg, D., and Kalkofen, D. (2017). Adaptive user perspective rendering for handheld augmented reality. In *2017 IEEE Symposium on 3D User Interfaces (3DUI)*, pages 176–181.
- Pucihar, K., Coulton, P., and Alexander, J. (2013). Evaluating dual-view perceptual issues in handheld augmented reality: Device vs. user perspective rendering. pages 381–388.

- Samini, A. and Palmerius, K. (2014). A perspective geometry approach to user-perspective rendering in handheld video see-through augmented reality.
- Sawilowsky, S. S. (2009). New effect size rules of thumb. In *Journal of Modern Applied Statistical Methods*, volume 8, pages 597–599.
- Shapiro, S. S. and Wilk, M. B. (1965). An analysis of variance test for normality (complete samples). *Biometrika*, 52(3/4):591–611.
- Tomioka, M., Ikeda, S., and Sato, K. (2013). Approximated user-perspective rendering in tablet-based augmented reality. In *2013 IEEE International Symposium on Mixed and Augmented Reality (ISMAR)*, pages 21–28.
- Uchida, H. and Komuro, T. (2013). Geometrically consistent mobile ar for 3d interaction. pages 229–230.
- Yoshida, T., Kuroki, S., Nii, H., Kawakami, N., and Tachi, S. (2008). *Arscope*. page 4.
- Zhang, E., Saito, H., and de Sorbier, F. (2013). From smartphone to virtual window. In *2013 IEEE International Conference on Multimedia and Expo Workshops (ICMEW)*, pages 1–6.

